

## Honeycomb catalysts for clean-up of diesel exhausts based upon the anodic-spark oxidized aluminum foil

S.F. Tikhov<sup>a</sup>, G.V. Chernykh<sup>a</sup>, V.A. Sadykov<sup>a,\*</sup>, A.N. Salanov<sup>a</sup>, G.M. Alikina<sup>a</sup>,  
S.V. Tsybulya<sup>a</sup>, V.F. Lysov<sup>b</sup>

<sup>a</sup> Borekov Institute of Catalysis SD RAS, pr. Lavrentieva 5, Novosibirsk, 630090, Russia

<sup>b</sup> Institute of Applied Physics, Novosibirsk, Russia

### Abstract

The technology of the aluminum foil anodic spark oxidation in the water-based electrolytes has been applied to form strongly adhering protective alumina layer at the surface. Basic features of the oxidation were studied by SEM and XRD. Secondary supports, promoters and modifiers including rare-earth elements were used to increase the thermal stability of these composites up to 900°C. These materials were assembled as thin wall honeycomb supports loaded with a number of active components. The catalysts were tested in the reactions of CO and CH<sub>x</sub> oxidation, NO<sub>x</sub> selective reduction by hydrocarbons and demonstrated a high performance and a low pressure drop at high space velocities. City diesel buses field tests of converters equipped with those catalysts demonstrated their high and stable performance in clean-up of exhausts from SOF, CO, gaseous hydrocarbons and NO<sub>x</sub>. ©1999 Elsevier Science B.V. All rights reserved.

### 1. Introduction

Control of diesel emissions is currently being addressed worldwide. Due to a rather low temperature of diesel exhausts usually not exceeding 400–500°C, requirements to the thermal stability of catalysts are less tough as compared with those for gasoline fueled automobiles. Further, these catalysts are due to oxidize the soluble organic fraction of particulates (SOF) present in the exhausts along with CO and CH<sub>x</sub>, and to reduce NO<sub>x</sub> in an excess of oxygen [1]. These functions can be distributed between the different types of active components, either finely intermixed to form a multifunctional catalyst [2–4] or spatially separated within the converter [5–6]. To achieve high conver-

sions at rather low operating temperatures, moderate GHSV, i.e., large catalysts volumes are required. To ensure a low pressure drop, the big diameter honeycomb monolith catalysts are the most promising. For this application, oxidized aluminum foil can be used as a suitable construction material. This presentation considers the design and testing of honeycomb catalysts based upon this type of supports.

### 2. Experimental

Aluminum foil with a thickness of 0.2–0.3 mm was anodic-spark oxidized as in [7] at a constant current density with a subsequent air calcination at 600°C for 2 h. The honeycomb structure was mainly shaped by stacking flat and corrugated sheets of foil and winding them into the Arkhimed spiral. In such a way,

\* Corresponding author. Tel.: +7-383-234-4682; fax: +7-383-234-3766

E-mail address: sadykov@catalysis.nsk.su (V.A. Sadykov)

triangular channels were formed. To enhance the exhaust stream turbulence, two corrugated sheets with slightly misaligned grooves forming while stacked criss-crossing channels were used in a proprietary design. After monolithic carriers shaping, they were washcoated by a secondary support based upon the hydrated alumina [7]. This procedure includes the next stages:

1. Thermal stabilization of the primary oxidic layer by impregnating it with lanthanum nitrate solution followed by calcination at 600°C for 1 h;
2. Monoliths impregnation by a water suspension of ceria-modified  $\gamma$ -alumina followed by drying at 120°C for 4 h and calcination at 600°C for 2 h.

The overall content of rare-earth elements in the secondary support layer was in the range of 20–25 wt.% as calculated on oxides.

Active components were introduced into the secondary support either by its impregnation with solutions of various precursors (platinum group metals, loading less than 0.15 wt.% [8]; manganese oxides, loading up to 2.5 wt.% [9]) or by adding preliminary synthesized fine powders (Cu-Sr/ZSM-5 [10] and mixed La-Ce-Cu perovskite-like system [11];) into alumina-based suspension (~25 wt.% with respect to alumina) at the washcoating stage (vide supra) followed by drying and calcination at 600 C for 2 h.

To carry out the field tests, a diesel converter with a volume ~11.5 l designed on the bases of a standard 'Ikarus' city bus muffler was manufactured. This converter was equipped with five pieces of big (diameters up to 18 cm) flow-through high cell density monoliths of different catalytic functions stacked consecutively in a proprietary sequence. Based upon the known approaches [2–6], the active components of these pieces (vide supra) were chosen as to ensure SOF and soot trapping; NO oxidation into NO<sub>2</sub>; interaction of NO<sub>2</sub> with adsorbed particulates to produce the products of their partial as well as deep oxidation; selective reduction of NO<sub>x</sub> in oxygen excess by hydrocarbons and oxygenates, oxidation of CO and VOC into CO<sub>2</sub> and H<sub>2</sub>O.

Catalytic activity in the reaction of NO<sub>x</sub> selective reduction by propane was determined in the integral flow reactor at GHSV = 50,000/h and the initial reaction mixture composition (vol.%): 0.1NO<sub>x</sub> + 0.13C<sub>3</sub>H<sub>8</sub> + 1.0O<sub>2</sub>, balance He. The catalytic activity in the reaction of butane (steady state

concentration of C<sub>4</sub>H<sub>10</sub> in air 0.2 vol. %) and CO oxidation (initial concentration of CO in air — 1.0 vol. %) were determined in the batch-flow gradientless kinetic installation. These measurements were carried out for pieces of micromonoliths made by the same procedure as described above, and GC was used to analyze the reaction mixture composition.

The diesel exhaust NO<sub>x</sub>, CO and VOC emissions during pilot and field tests were measured using a IMR 3000 P analyzer. The particulate content was characterized by the 'smoke' level determined according to the procedure set by requirement of the Russian Federation standards GOST 21393-75.

The process of the primary and secondary alumina oxide formation was studied by using SEM (BS-350 'Tesla') and XRD (URD-6 with monochromatic Cu K $\alpha$  radiation). Specific surface area was estimated by adsorption of Ar.

### 3. Results

#### 3.1. Design of supports and catalysts

To ensure the high adhesion and a reasonable thickness of the primary oxidic layer formed at the aluminum foil surface during the anodic-spark oxidation, the basic features of its formation were studied and optimized. As compared with the traditional anodic oxidation, the technology used here enabled to receive a thicker (5–10  $\mu$ m) oxidic layer with much lower porosity which covers all the surface thus protecting it from further oxidation at high temperatures [7]. According to the X-ray diffraction data, the primary oxidic layer is mainly comprised of a low-temperature  $\gamma$ -alumina phase characterized by its typical 220 and 440 reflections. Besides, aluminum phosphates are present as evidenced by diffraction peaks corresponding to 4.14 and 4.44 Å lattice spacing of different phosphate phase (Fig. 1). These admixtures can appear due to a capture of phosphate anions by the freshly formed anodic layer [12]. According to SEM data, the primary oxidic layer possesses cylindrical pores of 1–2  $\mu$ m in diameter, estimated concentration being equal to  $\sim 10^5$  pores/cm<sup>2</sup> [7]. The water capacity of aluminum support covered by this primary oxide layer is equal to  $\sim 0.07$  ml/g, specific surface area being around 0.1 m<sup>2</sup>/g.

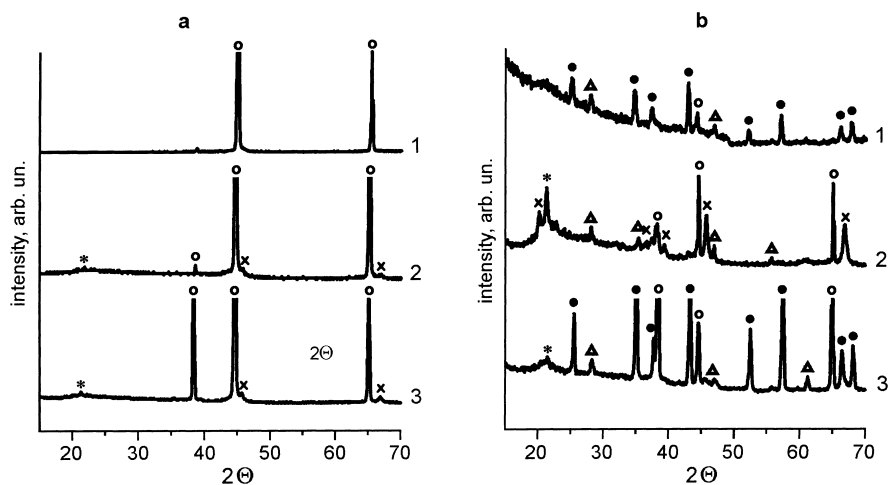


Fig. 1. X-ray diffraction patterns of different samples of aluminum foil: (a) as received, (b) after calcination in air at 900°C for 1 h; (1) unprotected aluminum foil; (2) with primary oxide layer; (3) with secondary oxide layer. Designation of reflections: aluminum (○),  $\gamma$ - $\text{Al}_2\text{O}_3$  (×), aluminum phosphates (\*),  $\alpha$ - $\text{Al}_2\text{O}_3$  (●), unknown (Δ).

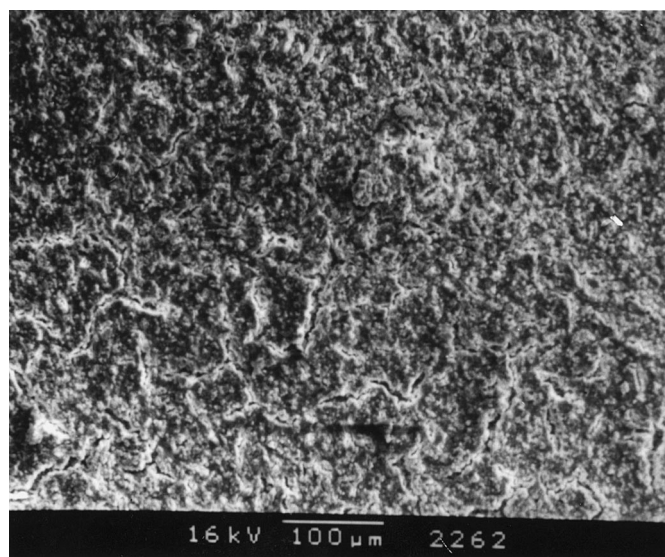


Fig. 2. SEM micrographs of aluminum foil with the secondary oxidic layer.

After the secondary alumina support washcoating, the specific surface reached 5–17 m<sup>2</sup>/g, and water capacity was increased to 0.15–0.25 ml/g that is sufficient for the practical application. For this system, the X-ray diffraction pattern demonstrates the same features as for the primary oxidic layer (Fig. 1). SEM image of the secondary washcoat is presented in Fig. 2. The average thickness of the secondary oxidic layer

is ~20–50 μm depending on the amount of supported alumina [8]. Taking into account that aluminum foil thickness is less than 300 μm, support designed here can be termed as layered, sandwich-type metalloce-ramic composite.

To preserve the shape of winded monolith, a stainless steel cylindrical cover was used. A general view of the honeycomb structure thus obtained is presented

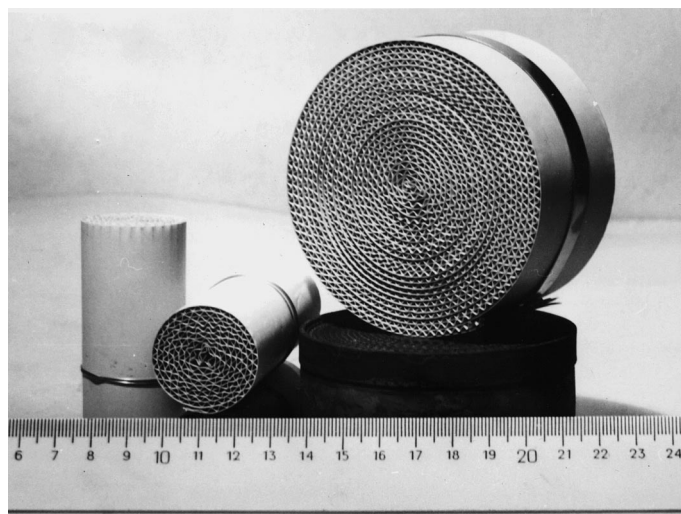


Fig. 3. Samples of aluminum foil-based monolithic supports.

in Fig. 3. The apparent density of these monoliths was  $\sim 1$  g/ml.

### 3.2. The catalysts thermostability

Earlier [13,14], similar composites prepared by traditional anodic oxidation of aluminum foil were shown to be suitable for preparation of highly active supported deep oxidation catalysts. Those catalysts can be promising for a number of new applications including a catalytic coating on a car's radiator and air conditioner condensers made of aluminum alloys [15]. However, thermal stability of these composites was not studied systematically. Meanwhile, for diesel converters, despite moderate average temperature of the exhaust, the problem of overheating is also of importance [16]. Due to the low melting point of aluminum, it could result in the destruction of the aluminum-containing composites. Hence, the thermal stability of these supports must be verified and, if required, improved.

For three types of aluminum foils: unprotected, anodic-spark oxidized and that covered with a secondary support, the effect of the air annealing at  $900^\circ\text{C}$  for 0.5 h has been studied. For the first one, after oxidation, the X-ray diffraction revealed accumulation of  $\alpha\text{-Al}_2\text{O}_3$  phase, while the intensity of aluminum peaks declined (cf. Fig. 1a and b). The aluminum foil protected by the primary oxide layer was

less sensitive to oxidation: the alumina phase composition was not changed, and intensities of aluminum diffraction peaks remained rather high (Fig. 1). The gravimetric estimations revealed that in these experiments, a degree of the aluminum oxidation declined from 80–90% for the initial foil to 10–15% for the foil protected by the anodic layer. Hence, the primary oxide layer greatly improves the thermal stability of aluminum. In part, it can be assigned to the ability of such a layer to maintain its phase composition and, hence, to remain compact, thus preventing the air contact with a molten aluminum. It is worth noting that  $\gamma\text{-alumina}$  supported from the suspension is less thermally stable and is converted into the corundum phase after annealing at  $900^\circ\text{C}$  (Fig. 1).

A dense protective oxide layer on the surface of aluminum was found to affect the mechanism of the aluminum oxidation. For non-protected aluminum foil oxidized at  $900^\circ\text{C}$ , oriented edge-on grown oxide platelets were nucleated at surface steps arranged in a spiral pattern decorating thus, probably, outlets of screw dislocations (Fig. 4a). This microstructure of the aluminum-alumina interface does not hinder aluminum oxidation. For the foil protected by the anodic layer, the molten aluminum appears to be transported through the pores to the surface and oxidized here. As the result, volcano-shaped cones are formed at pores outlets, elongated oxide particles accumulating nearby (Fig. 4b). Only weak variations in the surface

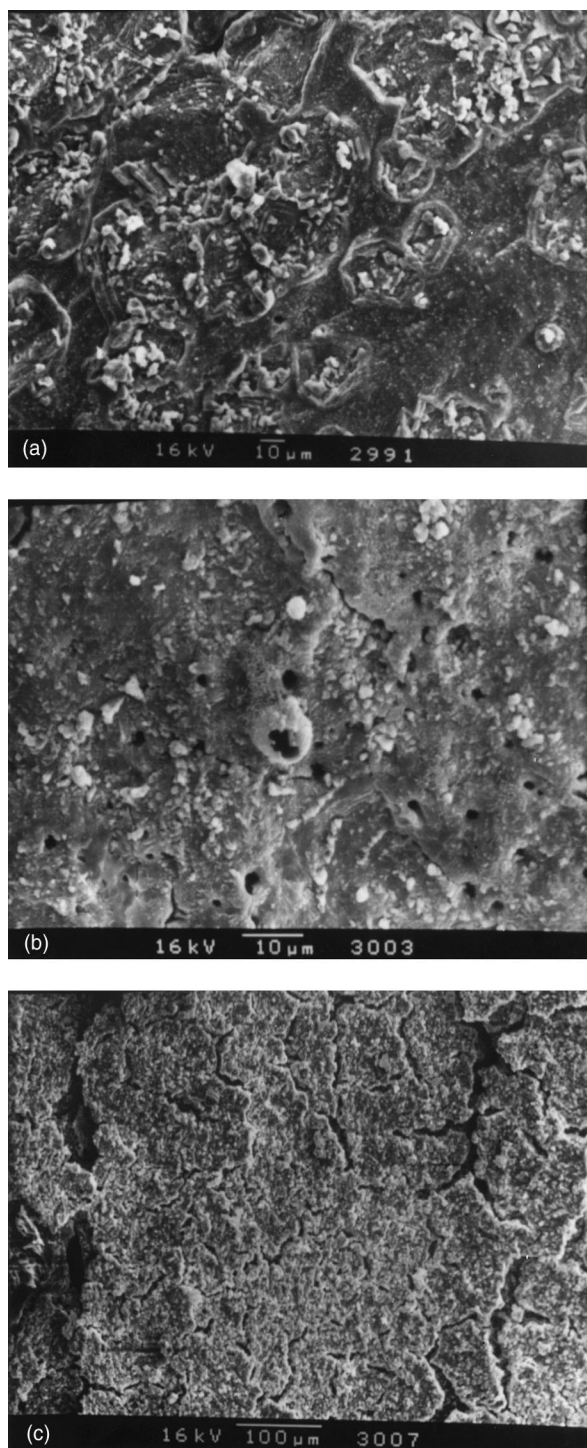


Fig. 4. SEM micrographs of different samples of aluminum foil after calcination at 900°C for 1 h: (a) unprotected aluminum foil; (b) with anodic oxide layer; (c) with secondary oxide layer.

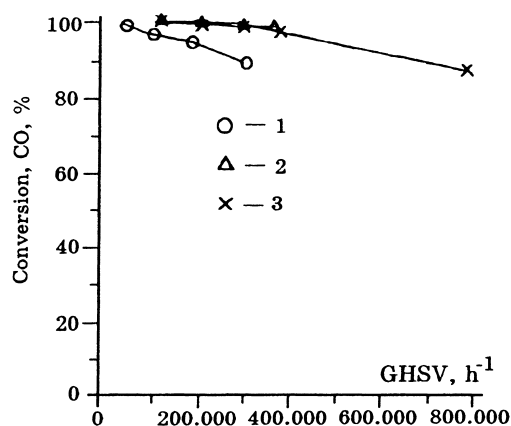


Fig. 5. CO conversion vs. space velocity for honeycomb catalysts with different active components: (1) Pd from Cl-containing precursor, (2) Pd from precursor without Cl, (3) Pt, Pd, Rh. Initial composition of reaction mixture 1 vol. % CO in air. Temperature 300°C. Total concentration of precious metals  $\sim 0.2$  wt. %.

microstructure were observed for the foil with the secondary alumina layer (Fig. 4c), though in this case  $\gamma \rightarrow \alpha$  transformation proceeds.

Hence, the anodic layer protects the aluminum foil from oxidation and leakage in the molten state. As the result, the composite integrity and honeycomb structure endured a short overheating. A reasonable thermal stability of this ceramometal carrier helps to retain an acceptable level of activity for supported catalysts (vide infra).

### 3.3. Catalytic activity

To meet future European emission requirements for diesel exhausts, converters are to remove CO, VOC, NO<sub>x</sub> and particulates [17]. Hence, various types of active components supported onto monolithic carriers made of anodic-spark oxidized aluminum foils were tested in the reactions of deep oxidation and NO<sub>x</sub> reduction using bench-scale installations and model mixtures.

Fig. 5 demonstrates performance of precious metals-containing catalysts in the reaction of CO oxidation. These data clearly show very high CO conversion at high GHSV at moderate loadings of precious metals. In comparison with traditional precious metal catalysts supported onto monolithic cordierite carriers [8], performance is clearly better which can be

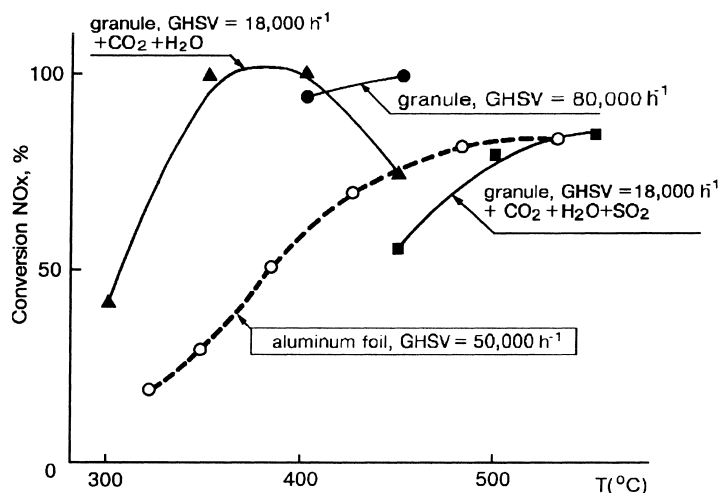


Fig. 6. Conversion of  $\text{NO}_x$  in the selective reduction by propane vs temperature for bulk and supported Cu-Sr/ZSM5 catalyst. The initial reaction mixture composition (vol. %): 0.1  $\text{NO}_x$  + 0.13  $\text{C}_3\text{H}_8$  + 1.0  $\text{O}_2$  + He. Additional reaction mixture components: + $\text{CO}_2$  — 5.0 vol. %  $\text{CO}_2$ ; + $\text{H}_2\text{O}$  — 5.0 vol. %  $\text{H}_2\text{O}$ ; + $\text{SO}_2$  — 700 ppm  $\text{SO}_2$ . Granule — granulated catalyst, foil-catalyst loaded on foil.

tentatively assigned to a specific morphology of the alumina layer [7].

In the reaction of butane oxidation, the catalysts supported onto aluminum foil-based carrier have also demonstrated good and stable performance. For samples calcined at 500°C, the rate of butane oxidation measured at 400°C varied in the range from  $7.9 \times 10^{-2}$  ml  $\text{C}_4\text{H}_{10}/\text{g s}$  (Pd-containing catalyst) to  $4.6 \times 10^{-2}$  ml  $\text{C}_4\text{H}_{10}/\text{g s}$  (Mn-containing catalyst). This range of activity is typical for the most active catalysts of deep oxidation including alumina supported precious metals and bulk transition metal oxides and perovskites [8,18]. After overheating at 700°C for 1 h, the reaction rate only slightly decreased for Pd-containing sample (to  $4.6 \times 10^{-2}$  ml  $\text{C}_4\text{H}_{10}/\text{g s}$ ), decline being more prominent for Mn-based active component (to  $1.2 \times 10^{-2}$  ml  $\text{C}_4\text{H}_{10}/\text{g s}$ ), though activity remained reasonably high. A special experiments for hydrothermal treatment of Pd-containing catalyst (18 h, 500°C, 42 vol. %  $\text{H}_2\text{O}$ ) have demonstrated its stability in these conditions, the activity being unchanged.

Fig. 6 shows typical performance features of a Cu-Sr/ZSM5 based catalysts used here as a middle-temperature catalyst of  $\text{NO}_x$  selective reduction by hydrocarbons [10], both supported onto the foil and tested as 1–2 mm granules. Strontium addi-

tion helped to suppress the irreversible deactivation of Cu-ZSM-5 caused by steaming [10,19]. This active component demonstrates high  $\text{NO}_x$  conversion even in the presence of water and carbon dioxide. High concentration of sulfur dioxide (700 ppm) not met in the diesel exhausts (usually around 20 ppm) clearly decreases activity, though it remains acceptable at higher temperatures. For supported catalyst, the activity is lower due to a lower content of the active component combined with the alumina-based binder within secondary support layer (vide supra).

### 3.4. Converter performance

Fig. 7 demonstrates the GHSV dependence of the pressure drop for designed converter. As follows from these data, at GHSV  $\sim 60,000$  h the pressure drop is around 0.12 bar not exceeding the design target for the diesel catalyst assembly [20]. For the converter volume used here (11.5 l), this GHSV value corresponds to the maximum volume flow rate  $\sim 720$  m<sup>3</sup>/h of the 'Ikarus' city bus [20].

A pilot test for converter equipped only with monoliths designed for oxidation of CO and VOC (Pd supported onto ceria-stabilized secondary alumina layer) in the real exhaust gases of diesel 'Ikarus' city bus has

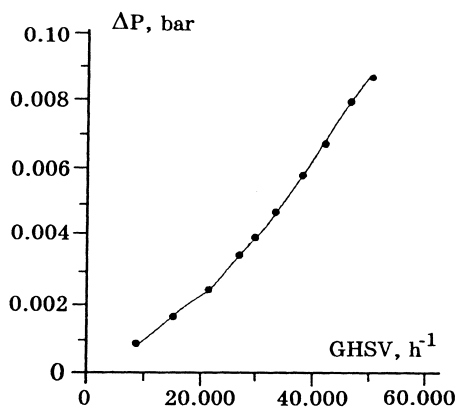


Fig. 7. The pressure drop–GHSV dependence for the converter equipped with five pieces of aluminum foil-based honeycomb catalyst. Overall catalysts volume  $\sim 11.5$  l, diameter — 180 mm.

shown that at inlet temperatures  $\sim 350^\circ\text{C}$  and GHSV  $\sim 200,000/\text{h}$ , CO conversion was  $\sim 83\%$ , and that of VOC  $\sim 64\%$ .

Prolonged field tests of catalytic converters equipped with five monolithic pieces designed for SOF, HC and CO oxidation and  $\text{NO}_x$  selective reduction have been carried out in Moscow. Those converters installed at city buses have demonstrated a good performance removing  $\sim 70$ – $80\%$  of SOF, CO and HC, and at least  $50\%$  of  $\text{NO}_x$  during four months of trials successfully continued at present.

#### 4. Discussion

Catalytic clean-up of diesel exhausts is known to be a more complex problem as compared with those of gasoline engines. Due to admixture of sulfur in the diesel fuel, oxidation of SOF and dry soot on precious metal containing catalysts could generate undesirable emission of  $\text{SO}_3$  and sulfuric acid [21]. Traditional three-way catalysts fail to reduce  $\text{NO}_x$  in exhausts with high oxygen content. The most successful were efforts aimed at developing catalysts for removal of SOF, VOC and CO from diesel exhausts [21–23]. The addition of a proprietary zeolite as a hydrocarbon trap and a small amount of Pt to the platform  $\text{CeO}_2$  catalyst enables European emission standards for CO, HC and particulates to be met [22]. To increase the  $\text{NO}_x$  selective reduction performance, combination of sup-

ported precious metals with cation-exchanged zeolites and transition metal oxides or perovskites is suggested [2–6].

The last trends in the design of diesel exhaust converters are oriented on flow-through high cell density (up to 400 cpsi) monolithic catalysts of a big (18–26 cm) cross-section [22]. In such monoliths, a laminar gas flow regime is realized. The volume of monoliths is usually close to the displacement volume of cylinders, while concentration of supported precious metals ( $0.5$ – $2.0 \text{ g/ft}^3$ ) is substantially lower than that for the three-way catalysts [1].

All these trends were taken into account in our design of catalytic converter with monoliths catalysts based upon the oxidized and thermally stabilized aluminum foil. As judged by the results of field tests, the combination of the active components used here is at least very promising for simultaneous removal of particulates, HC, CO and  $\text{NO}_x$ . All previous designs of diesel converters were not able to ensure the  $\text{NO}_x$  abatement [1]. The origin of such efficiency clearly deserves some comments.

First of all, due to a higher flexibility of alumina foils as compared with ceramic and stainless steel supports, a criss-crossing channel pattern is easily formed which helps to make the gas flow turbulent. As the result, particulates were trapped in the monolith channels during cold-start regimes when particulates and NO emission is the highest [17]. A part of hydrocarbons is trapped in zeolite. Simultaneously, NO oxidation into  $\text{NO}_2$  effectively catalyzed by transition metal oxides [3] and supported precious metals [6] helps to fix  $\text{NO}_x$  as adsorbed nitrite–nitrate species. The monolithic pieces with such functions were situated at the inlet part of the converter. At the stationary regimes of high speed, hard acceleration driving, when high temperatures of exhaust are achieved [17], trapped carbonaceous materials are easily oxidized by adsorbed  $\text{NO}_x$  species or gaseous  $\text{NO}_2$  yielding mainly NO, and NO is reoxidized back into  $\text{NO}_2$  thus maintaining a cycle of particulates oxidation [24]. Such an oxidation of SOF in the adlayer or within zeolite channels yields a lot of partial oxidation products including aldehydes, alcohols, olefins etc. known to be very efficient in NO selective reduction in oxygen excess catalyzed by supported precious metals [25], Cu-ZSM-5 [26] and alumina [5,27] even in the presence of small (ca 20 ppm) admixture of sulfur dioxide. Combination

of low-temperature (supported precious metals) and middle-temperature (Cu-ZSM-5, Ce-alumina system) catalysts of NO<sub>x</sub> reduction helps to expand the operation temperature window [5,28]. In such a way, problems connected with too low concentrations of VOC in the diesel exhaust to ensure the efficient NO<sub>x</sub> reduction appear to be at least partially overcome. The monolithic pieces with this function were installed at the middle part of the converter. At last, CO oxidation into CO<sub>2</sub> was effectively catalyzed by the monolithic piece with supported Pd situated at the converter outlet.

## 5. Conclusions

Monolithic supports based upon the anodic-spark oxidized and thermally stabilized aluminum foil wash-coated by a secondary alumina layer are elaborated. Perovskites, rare-earth and transition metal oxides combined with precious metals were used as active components of the multifunctional catalysts promising for the four-way diesel exhaust gases clean-up. City bus converters equipped with those catalysts have successfully passed the field tests.

## References

- [1] R.M. Heck, R.J. Farrauto, Catalytic air pollution control. Commercial Technology, Van Nostrand Reinhold, New York, 1995, p. 113, 161.
- [2] T. Maunula, Y. Kintaichi, M. Inaba, K. Sato, H. Hamada, Appl. Catal. B 15 (1998) 291.
- [3] M. Misono, Cat. Tech. 4 (1998) 183.
- [4] J.C. Menezes, S. Inkari, T. Bertin, J. Barbier, N. Davias-Bainier, R. Noirot, T. Seguelong, Appl. Catal. B 15 (1998) L1.
- [5] A. Obuchi, I. Kaneko, J. Oi, A. Ogata, G.R. Bamwenda, S. Kushiya, Appl. Catal. B 15 (1998) 37.
- [6] M. Iwamoto, T. Zengyo, A.M. Hernandez, H. Araki, Appl. Catal. B 17 (1998) 256.
- [7] S.F. Tikhov, G.V. Chernykh, V.A. Sadykov, A.N. Salanov, S.V. Tsybulya, G.M. Alikina, V.F. Lysov, in: Mater. Res. Soc. Symp. Proc. Ser. (Recent Advances in Catalytic Materials), MRS, Warrendale, PA, 1998, vol. 497, p.71.
- [8] G.V. Chernykh, Z.R. Ismagilov, R.A. Shkrabina, A.V. Kalinkin, in: Congr. Proc. 3rd Int. Symp. Catalysis and Automotive Pollution Control (CAPOC3), Preprints, Brussel, 20–22 April 1994, Paper No. 26, vol. 2, p. 245.
- [9] Patent RU No. 2103057.
- [10] Patent RU No. 2088316.
- [11] Patent RU No. 2100067.
- [12] V.F. Surganov, A.M. Mozalev, N.N. Mozaleva, Russian J. Appl. Chem. 70 (1997) 267 (in Russian).
- [13] I.E. Sungkono, H. Kameyama, T. Koya, Appl. Surf. Sci. 121/122 (1997) 425.
- [14] N. Burgos, M. Paulis, J. Sambeth, J.A. Odriozola, M. Montes, Stud. Surf. Sci. Catal. (Preparation of Catalysts YII), Elsevier Science B.V. 1998, v.118, p.157.
- [15] J. Hoke, D. Anderson, R. Heck, T. Poles, J. Steger, SAE Paper No. 960800, 1996.
- [16] W. Tylus, K. Suszewska, A. Muzialik, J. Zabrevski, in: Abstracts of Proc. 2nd Int. Seminar on Monolith honeycomb supports and catalysts, Novosibirsk, 12–15 July 1997, Paper No 9.
- [17] K.M. Adams, J.V. Cavataio, R.H. Hammerle, Appl. Catal. B 10 (1996) 157.
- [18] V.A. Sadykov, L.A. Isupova, S.F. Tikhov, O.N. Kimkhai, in: Mater. Res. Soc. Symp. Proc. Ser. (Synthesis and Properties of Advanced Catalytic Materials), MRS, Pittsburgh, 1995, vol. 368, p. 293.
- [19] V.A. Sadykov, G.M. Alikina, R.V. Bunina, S.L. Baron, S.A. Veniaminov, V.N. Romannikov, V.P. Doronin, A. Ya. Rozovskii, V.F. Tretyakov, V.A. Matyshak, V.V. Lunin, E.V. Lunina, A.N. Kharlanov, Proc. 1st World Congr. Environmental Catalysis for a Better World and Life, Pisa, Italy, 1–5 May 1995, p. 315–318.
- [20] J.C. Clerc, Appl. Catal. B 10 (1996) 99.
- [21] K.E. Voss, J.K. Lampert, R.J. Farrauto, G.W. Rice, A. Panke, in: Congr. Proc. 3rd Int. Symp. on Catalysis and Automotive Pollution Control (CAPOC3), Preprints, Brussel, 20–22 April 1994, paper No 20, vol.1, p. 227.
- [22] R.J. Farrauto, K.E. Voss, Appl. Catal. B 10 (1996) 29.
- [23] J.E. Johnson, D.B. Kittelson, Appl. Catal. B 10 (1996) 117.
- [24] G. Mui, W. Zhu, F. Kapteijn, J.A. Moulijn, Appl. Catal. B, Environ. 17 (1998) 205.
- [25] R. Burch, T.C. Watling, Appl. Catal. 17 (1998) 131.
- [26] M. Iwamoto, Catal. Today 29 (1996) 29.
- [27] H. Hamada, Y. Kintaichi, M. Sasaki, T. Ito, T. Yoshinari, M. Tabata, H. Tsuchida, F. Suganuma, A. Kitazume, K. Usui, Shokubai 34 (1992) 364.
- [28] M. Haneda, Y. Kintaichi, M. Inaba, H. Hamada, Bull. Chem. Soc. Jpn. 70 (1997) 2171.